

See discussions, stats, and author profiles for this publication at: <https://www.researchgate.net/publication/261228778>

# Four-wave mixing in semiconductor optical amplifiers for high-speed communications

Conference Paper · December 2012

DOI: 10.1109/CODEC.2012.6509322

---

CITATIONS

4

---

READS

97

3 authors, including:



**Narottam Das**

Central Queensland University

102 PUBLICATIONS 640 CITATIONS

[SEE PROFILE](#)



**Mohammad Razaghi**

University of Kurdistan

59 PUBLICATIONS 160 CITATIONS

[SEE PROFILE](#)

Some of the authors of this publication are also working on these related projects:



MSM photodetector [View project](#)



Modeling and Analysis of Different Nano-gratings to Enhance Light Absorption in MSM-PDs [View project](#)

# Four-Wave Mixing in Semiconductor Optical Amplifiers for High-Speed Communications

Narottam Das  
Department of Electrical and  
Computer Engineering, Curtin  
University,  
Perth, WA 6845, Australia  
[narottam.das@curtin.edu.au](mailto:narottam.das@curtin.edu.au)

Mohammad Razaghi  
Department of Electrical and  
Computer Engineering,  
University of Kurdistan, Iran  
[m.razaghi@uok.ac.ir](mailto:m.razaghi@uok.ac.ir)

S. Rasoul Hosseini  
Department of Electrical  
Engineering, University of  
Wisconsin-Milwaukee,  
Milwaukee, WI, USA  
[rhosseini2005@gmail.com](mailto:rhosseini2005@gmail.com)

**Abstract**— This paper presents propagation characteristics of short optical pulses and four-wave mixing (FWM) in semiconductor optical amplifiers (SOAs) for high conversion efficiency. For the simulation of pulse propagation in SOA, the nonlinear propagation equation is used for taking into account the gain spectrum dynamics, gain saturation which depends on carrier depletion, carrier heating, spectral hole-burning, group velocity dispersion, self-phase modulation and two photon absorption. Finite-difference beam propagation method (FD-BPM) is used to solve the nonlinear Schrödinger equation and obtained the propagation characteristics of two optical pulses with different frequencies, which are simultaneously injected into the SOA.

**Key Words**— Finite-difference beam propagation method, FWM conversion efficiency, pulse propagation and wave mixing, semiconductor optical amplifier.

## I. INTRODUCTION

Four-wave mixing (FWM) is an important phenomenon in semiconductor optical amplifiers (SOAs), lasers and optical fibers for optical communication systems due to high speed data processing and high conversion efficiency [1]-[7]. Commonly, the FWM conversion efficiency in an SOA is limited due to gain saturation. However, the high FWM conversion efficiency can be achieved with the short optical pump and probe pulses because it is possible to reduce the gain saturation and increase of the FWM conversion efficiency in an SOA by using the strong pump intensity [1]-[7]. The analytical approach is indispensable in order to design high-efficient and high-speed FWM conversion devices and make the clear understanding about the fast nonlinear interaction process of FWM in SOAs.

The early reports have been used for the analyses of FWM among short optical pulses in SOAs but these are not sufficient, because they have not taken into account the group velocity dispersion and have not discussed the effects of the wavelength dependence of the gain in detail, which clearly appears for a large detuning [7]. The SOAs small size, high optical gain, low input power requirement, faster response time, large bandwidth and compatible optoelectronic characteristics have made the SOA very attractive element to be used in optical devices. The SOAs are useful to amplify short pulses and to

contribute in ultrahigh-speed optical communication systems [3-7].

The main objective of this paper is to investigate the nonlinear optical pulse propagation and FWM in SOAs for high speed communication systems. This analysis is based on the nonlinear Schrödinger equation considering self-phase modulation (SPM), two-photon absorption (TPA), group velocity dispersion (GVD), carrier depletion, carrier heating, spectral-hole burning (SHB), gain spectrum dynamics and gain saturation in an SOA [4, 9]. Finite-difference beam propagation method (FD-BPM) is used to solve the nonlinear Schrödinger equation because of short convergence time and excellent accuracy of the simulated results [4, 10-11]. This paper is organized as follow; Introduction is in section I, nonlinear effects in SOAs are in section II, theoretical model of SOAs is in section III. Section IV deals with simulation results and discussion. Finally the conclusions are presented in section V.

## II. NONLINEAR EFFECTS IN SOAS

The SOAs are a useful nonlinear device for high-speed communication systems. There are several/different types of “nonlinear effects” occur in the SOAs. The important four types of “nonlinear effects” are shown in Fig. 1. These are namely: (i) spectral hole-burning (SHB), (ii) carrier heating (CH), (iii) carrier depletion (CD) and (iv) two-photon absorption (TPA). For the modeling of wave propagation in the SOA, all of these effects are taken into account in the mathematical formulation of modified nonlinear Schrödinger equation (MNLSE) [4, 9].

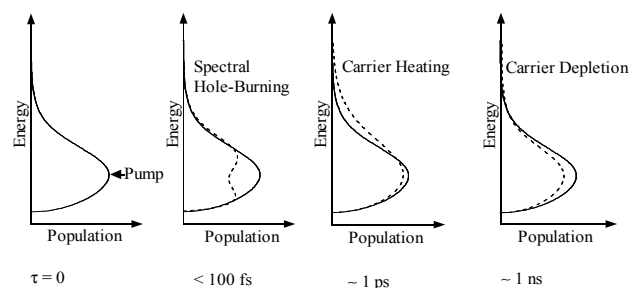


Figure 1. The important nonlinear effects in SOAs: (i) spectral hole-burning (SHB) with a life time of less than 100 fs (i.e.,  $< 100$  fs), (ii) carrier heating (CH) with a life time of  $\sim 1$  ps, (iii) carrier depletion (CD) with a life time is  $\sim 1$  ns and (iv) two-photon absorption (TPA).

Figure 1 shows the time-development diagram of the population density in the conduction band after excitation [10]. The excitation laser energy as pump (represented by

the arrow) shown in Fig. 1. When the life time is less than 100 fs (i.e., <100 fs), the SHB effect is dominant. The SHB occurs when a narrow-band strong pump beam excites the SOA, which has an inhomogeneous broadening. The SHB arises due to the finite value of intraband carrier-carrier scattering time ( $\sim 50$ -100 fs), which sets the time scale on which a quasi-equilibrium Fermi distribution is established among the carriers in a band. After the life time  $\sim 1$  ps, the SHB effect is relaxed and the CH effect becomes dominant. The “hot”-carriers relax to the lattice temperature through the emission of optical phonons with a relaxation time of  $\sim 0.5$ -1 ps. The effect of CD remains for about 1 ns. The stimulated electron-hole recombination depletes the carriers, thus reducing the optical gain. The band-to-band relaxation also causes CD, with a relaxation time of  $\sim 0.2$ -1 ns. For ultrashort optical pumping, the TPA effect also becomes important. An atom makes a transition from its ground state to the excited state by the simultaneous absorption of two laser photons. All these nonlinear effects (mechanisms) are taken into account in the MNLSE.

### III. THEORETICAL MODEL OF SOAS

The following MNLSE [4, 9] is used for the simulation of pulse propagation and FWM characteristics input pulses (such as, pump and probe pulses) in SOAs.

$$\left[ \frac{\partial}{\partial z} - \frac{i}{2} \beta_2 \frac{\partial^2}{\partial \tau^2} + \frac{\gamma}{2} + \left( \frac{\gamma_{2p}}{2} + i b_2 \right) |V(\tau, z)|^2 \right] V(\tau, z) = \left\{ \frac{1}{2} g_N(\tau) \left[ \frac{1}{f(\tau)} + i \alpha_N \right] + \frac{1}{2} \Delta g_T(\tau) (1 + i \alpha_T) - i \frac{1}{2} \frac{\partial g(\tau, \omega)}{\partial \omega} \Big|_{\omega_0} \frac{\partial}{\partial \tau} - \frac{1}{4} \frac{\partial^2 g(\tau, \omega)}{\partial \omega^2} \Big|_{\omega_0} \frac{\partial^2}{\partial \tau^2} \right\} V(\tau, z) \quad (1)$$

Here,  $\tau (= t - z/v_g)$  is the frame of local time, which propagates with a group velocity  $v_g$  at the center frequency of an optical pulse. A slowly varying envelope approximation is used in (1), where the temporal variation of the complex envelope function is very slow compared with the cycle of the optical field. In (1),  $V(\tau, z)$  is the time domain complex envelope function of an optical pulse,  $|V(\tau, z)|^2$  represents the corresponding optical pulse power, and  $\beta_2$  is the GVD.  $\gamma$  is the linear loss,  $\gamma_{2p}$  is the TPA coefficient,  $b_2 (= \omega_0 n_2 / cA)$  is the instantaneous SPM term due to the instantaneous nonlinear Kerr effect  $n_2$ ,  $\omega_0 (= 2\pi f_0)$  is the center angular frequency of the pulse,  $c$  is the velocity of light in vacuum,  $A (= wd/\Gamma)$  is the effective area ( $d$  and  $w$  are the thickness and width of the active region, respectively and  $\Gamma$  is the confinement factor) of the active region. The saturation of the gain due to the CD is given by

$$g_N(\tau) = g_0 \exp \left( - \frac{1}{W_s} \int_{-\infty}^{\tau} e^{-s/\tau_s} |V(s)|^2 ds \right) \quad (2)$$

where,  $g_N(\tau)$  is the saturated gain due to CD,  $g_0$  is the linear gain,  $W_s$  is the saturation energy,  $\tau_s$  is the carrier lifetime. The SHB function  $f(\tau)$  is given by

$$f(\tau) = 1 + \frac{1}{\tau_{shb} P_{shb}} \int_{-\infty}^{+\infty} u(s) e^{-s/\tau_{shb}} |V(\tau - s)|^2 ds \quad (3)$$

where,  $f(\tau)$  is the SHB function,  $P_{shb}$  is the SHB saturation power,  $\tau_{shb}$  is the SHB relaxation time, and  $\alpha_N$  and  $\alpha_T$  are the linewidth enhancement factor associated

with the gain changes due to CD and CH. The resulting gain change due to the CH and TPA is given by

$$\Delta g_T(\tau) = -h_1 \int_{-\infty}^{+\infty} u(s) e^{-s/\tau_{ch}} (1 - e^{-s/\tau_{shb}}) |V(\tau - s)|^2 ds - h_2 \int_{-\infty}^{+\infty} u(s) e^{-s/\tau_{ch}} (1 - e^{-s/\tau_{shb}}) |V(\tau - s)|^4 ds \quad (4)$$

where,  $\Delta g_T(\tau)$  is the resulting gain change due to the CH and TPA,  $u(s)$  is the unit step function,  $\tau_{ch}$  is the CH relaxation time,  $h_1$  is the contribution of stimulated emission and free-carrier absorption to the CH gain reduction and  $h_2$  is the contribution of TPA.

The dynamically varying slope and curvature of the gain plays a shaping role for pulses in the sub-picosecond range. The first and second order differential net (saturated) gain terms are

$$\begin{aligned} \frac{\partial g(\tau, \omega)}{\partial \omega} \Big|_{\omega_0} &= A_1 + B_1 [g_0 - g(\tau, \omega_0)] \\ \frac{\partial^2 g(\tau, \omega)}{\partial \omega^2} \Big|_{\omega_0} &= A_2 + B_2 [g_0 - g(\tau, \omega_0)] \\ g(\tau, \omega_0) &= g_N(\tau, \omega_0) / f(\tau) + \Delta g_T(\tau, \omega_0) \end{aligned} \quad (5)$$

where,  $A_1$  and  $A_2$  are the slope and curvature of the linear gain at  $\omega_0$ , respectively, while  $B_1$  and  $B_2$  are constants describing changes in  $A_1$  and  $A_2$  with saturation, as given in (5). The gain spectra of SOAs are very important for obtaining the propagation and FWM characteristics between pulses [3-4, 8-9].

### IV. SIMULATION RESULTS AND DISCUSSION

In this section simulation result of single pulse propagation and FWM characteristics are discussed. This model includes the dynamic gain change terms, i.e. the first- and second-order gain spectrum terms, which are the last two terms of the right side in (1). Therefore, it is not possible to separate the linear propagation term (GVD term) and phase compensation terms (other than GVD, first- and second-order gain spectrum terms). Therefore, it is not possible to use the common methods like the fast Fourier transformation BPM (FFT-BPM). Hence, the FD-BPM for the simulation method is used [4, 10-11].

#### A. Single Optical Pulse Propagation in SOAs

Optical pulse propagation in SOAs has drawn considerable attention due to its potential applications in high-speed optical communication systems, such as a wavelength converter based on FWM and switching.

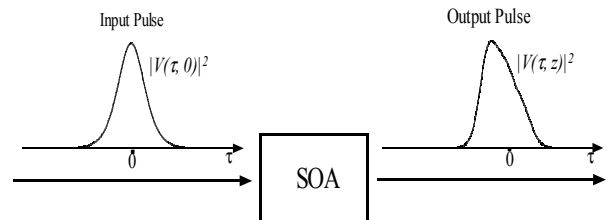


Figure 2. A simple schematic diagram for the simulation of nonlinear single pulse propagation in SOA.

Figure 2 illustrates a simple simulation model for nonlinear pulse propagation characteristics in an SOA. An optical pulse is injected into the input side of the SOA ( $z = 0$ ). Here,  $\tau$  is the local time,  $|V(\tau, 0)|^2$  is the intensity

(power) of input pulse ( $z = 0$ ) and  $|V(\tau, z)|^2$  is the intensity (power) of the output pulse after propagating a distance  $z$  at the output side of SOA. This model is used to simulate the FWM characteristics (with single probe) and wave-mixing (with multi-pump or probe pulses) characteristics in SOAs.

Table-I.

Bulk SOA parameters (AlGaAs/GaAs, double heterostructure) [4, 9].

Name of the parameters	Symbols	Values	Units
Length of SOA	L	500	$\mu\text{m}$
Effective area	A	5	$\mu\text{m}^2$
Center frequency of pulse	$f_0$	349	THz
Linear gain	$g_0$	92	$\text{cm}^{-1}$
Group velocity dispersion	$\beta_2$	0.05	$\text{ps}^2 \text{cm}^{-1}$
Saturation energy	$W_s$	80	pJ
Linewidth enhancement factor due to the CD	$\alpha_N$	3.1	
Linewidth enhancement factor due to the CH	$\alpha_T$	2.0	
Contribution of stimulated emission and FCA to the CH gain reduction	$h_1$	0.13	$\text{cm}^{-1} \text{pJ}^{-1}$
The contribution of TPA	$h_2$	126	$\text{fs cm}^{-1} \text{pJ}^{-2}$
Carrier lifetime	$\tau_s$	200	ps
CH relaxation time	$\tau_{ch}$	700	fs
SHB relaxation time	$\tau_{shb}$	60	fs
SHB saturation power	$P_{shb}$	28.3	W
Linear loss	$\gamma$	11.5	$\text{cm}^{-1}$
Instantaneous nonlinear Kerr effect	$n_2$	-0.70	$\text{cm}^2 \text{TW}^{-1}$
TPA coefficient	$\gamma_{2p}$	1.1	$\text{cm}^{-1} \text{W}^{-1}$
Parameters describing second-order Taylor expansion of the dynamically gain spectrum	$A_1$	0.15	$\text{fs } \mu\text{m}^{-1}$
	$B_1$	-80	fs
	$A_2$	-60	$\text{fs}^2 \mu\text{m}^{-1}$
	$B_2$	0	$\text{fs}^2$

Figure 3 shows the simulation results for single nonlinear optical pulse propagation in SOAs. The bulk SOA with the wavelength of  $0.86 \mu\text{m}$  parameters are listed in Table-I. Fig. 3(a) shows the temporal waveform of the propagated pulse for different output energy levels. For this simulation, the SOA length was selected  $500 \mu\text{m}$  and the input pulse width was 1 ps. With increasing the input pulse energy, the output pulse energy increased until it saturated the gain of the SOA. The peak position of the pulses are shifted towards the leading edge (negative time), which is mainly due to the gain saturation of the SOA [8], because the gain experienced by the pulses is higher at the leading edge than the trailing edge. Fig. 3(b) shows the spectral characteristics of the propagated pulse at the output of the SOA for different output energy levels. These spectral characteristics were obtained by using the fast Fourier transform (FFT) of the temporal waveforms (or pulse shapes) as shown in Fig. 4(a). From Fig. 4(b), it also noticed that by increasing the input pulse energy, the output pulse energy increases until the SOA is driven into saturation. The dips observed at the higher frequency side of the frequency spectra are due to the self-phase modulation characteristics of the SOA [8]. It also noticed that the output frequency spectra are red-shifted (the spectral peak positions are slightly shifted to the lower frequency side of the frequency spectra), and this is also attributed to the gain saturation of the SOA [8]. The

simulation results are in excellent agreement with the experimental results reported [8].

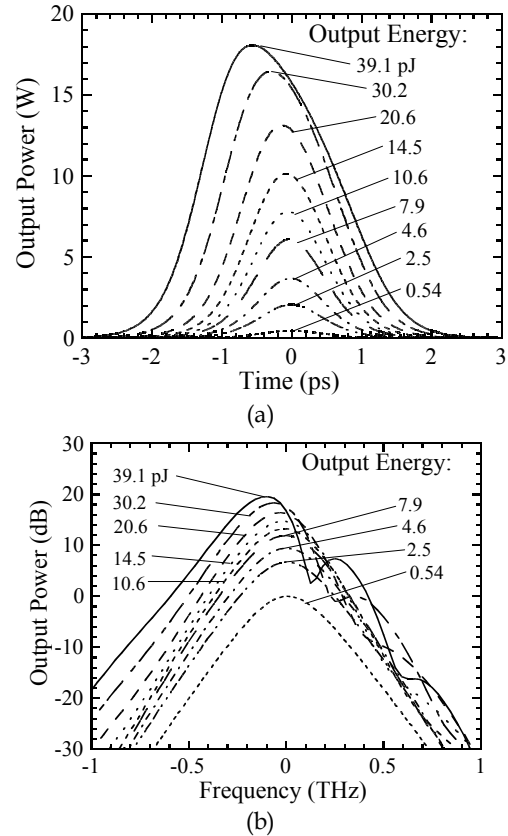


Figure 3. (a) Temporal waveform of the propagated pulses at the output of the SOA. Input pulse-width is 1 ps. (b) Spectral waveform of the output pulses at different output energy levels.

### B. FWM (Propagation of two input pulses) in SOAs

When two optical pulses with different central frequencies of  $f_p$  (pump) and  $f_q$  (probe) are injected into the SOA simultaneously, the FWM signal is generated in the SOA at a frequency of  $2f_p - f_q$ . For the analysis of the nondegenerate FWM characteristics, we use the following equation for describing the two input (pump and probe) pulses, which are simultaneously injected into the SOA [4].

$$V(\tau) = V_p(\tau) + V_q(\tau) \exp(-i\Delta\omega\tau) \quad (6)$$

where,  $V_p(\tau)$  and  $V_q(\tau)$  are the complex envelope functions of the input pump and probe pulses, and  $\Delta\omega$  is the angular frequency detuning between pump and probe pulses, expressed as  $\Delta\omega = 2\pi\Delta f = 2\pi(f_p - f_q)$ . Using the complex envelope function of (6), get the solution of (1) for two pulses propagation characteristics and obtain the FWM signal in the SOA.

Fig. 4(a) shows the output spectrum of the SOA for weak input pulse energy. The pulsewidths of input two (pump and probe) pulses are 10 ps. The input pump and probe pulse energies are 10 fJ and 1 fJ, respectively. The pump-probe detuning is +1 THz. The gain does not saturate with this input energy. It shows that the output and input frequency spectra, which were obtained by performing a fast Fourier transformation of the temporal pulses. The horizontal axis is the difference frequency from the central frequency of pump pulse ( $f_0 = 349 \text{ THz}$ ).

The vertical axis is the power normalized at the power of the central frequency of the input pump pulse. The new signal is found in the output spectrum, whose peak position satisfies the relation of  $2f_p - f_q$ . This signal is generated by the FWM process in an SOA. The output pump pulse, output probe pulse and the generated FWM signals are shown for different SOA lengths.

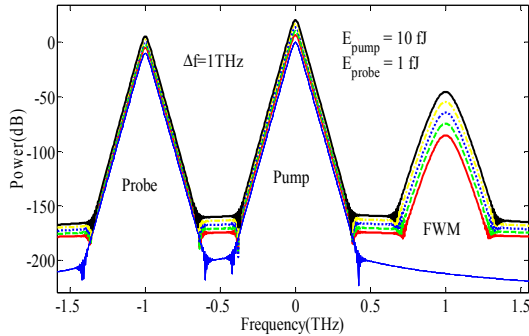


Figure 4(a). Frequency spectra of the input (pump and probe,  $z=0$ ) and output pulses (pump, probe and generated signals,  $z=400, 450, 500, 550, 600$   $\mu\text{m}$ ). Where,  $\Delta f = +1$  THz is the detuning frequency.

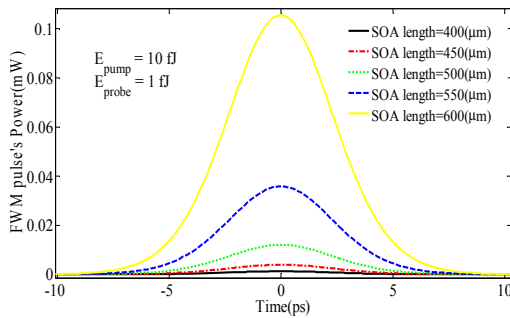


Figure 4(b). The waveform of the generated FWM signals for various SOA lengths as shown the spectra in Fig. 4(a).

Fig. 4(b) shows the generated FWM signals for different SOA lengths as mentioned above as well as in the legend. The output spectrum of Fig. 4(a) is filtered from -500 to +500 GHz of the FWM signal's central frequency of  $2f_p - f_q$  and performed an inverse Fourier transform of their respective components. In the case of relatively weak input energy, the pulsewidth of the FWM signal becomes narrow because the FWM signal intensity is proportional to  $I_p^2 I_q$ . Here,  $I_p$  is the pump pulse intensity and  $I_q$  is the probe pulse intensity. The peak positions of all the pulses remain at  $t = 0$  because the GVD effect is small under these conditions [4]. From the above results, it shows clearly that the FWM signal the power (energy) increases with the increase of SOA lengths. Here,  $G_0 = \exp(g_0 L)$  is the unsaturated gain of the SOA and it has exponential relation to the length of the SOA. So, with increasing the SOA length leads to more amplified output pulse energy.

## V. CONCLUSIONS

The propagation characteristics of short optical pulses in an SOA are analyzed by using the FD-BPM. In the

output waveform, it was observed that the peak positions are shifted to the leading edge, which is due to the gain saturation of the SOA. The output spectra are red-shifted and the dips are observed at the higher frequency side of the spectra. Also, the nondegenerate FWM characteristics between short optical pulses in SOAs are analyzed. From simulation results, it is clear that the FD-BPM is a very useful technique for simulating the FWM characteristics in SOAs. Therefore, this method is extremely useful for the design of high efficiency wavelength converters, wavelength division multiplexers, and optical phase conjugators for high-speed communications in SOAs.

## ACKNOWLEDGMENT

This research is supported by Faculty of Science and Engineering, Curtin University, Perth, WA, Australia.

## REFERENCES

- [1] M. Shtaf and G. Eisenstein, "Analytical solution of wave mixing between short optical pulses in semiconductor optical amplifier," *Appl. Phys. Lett.*, vol. 66, pp. 1458-1460, 1995.
- [2] M. Shtaf, R. Nagar, and G. Eisenstein, "Four-wave mixing among short optical pulses in semiconductor optical amplifiers," *IEEE Photon. Technol. Lett.*, vol. 7, pp. 1001-1003, 1995.
- [3] J. Inoue and H. Kawaguchi, "Highly nondegenerate four-wave mixing among subpicosecond optical pulses in a semiconductor optical amplifier," *IEEE Photon. Technol. Lett.*, vol. 10, pp. 349-351, 1998.
- [4] N. K. Das, Y. Yamayoshi, and H. Kawaguchi, "Analysis of basic four-wave mixing characteristics in a semiconductor optical amplifier by beam propagation method," *IEEE J. Quantum Electron.* vol. 36, Oct. 2000.
- [5] C. Xie, P. Ye, and J. Lin, "Four-wave mixing between short optical pulses in semiconductor optical amplifiers with the consideration of fast gain saturation," *IEEE Photon. Technol. Lett.*, vol. 11, pp. 560-562, May 1999.
- [6] A. Mecozzi, A. D'Ottavi, E. Iannone, and P. Spano, "Four-wave mixing in travelling-wave semiconductor amplifiers," *IEEE J. Quantum Electron.*, vol. 31, pp. 689-699, 1995.
- [7] A. Mecozzi and J. Mørk, "Saturation effects in nondegenerate four-wave mixing between short optical pulses in semiconductor laser amplifiers," *IEEE J. Select. Topics Quantum Electron.*, vol. 3, pp. 1190-1207, 1997.
- [8] H. Kawaguchi, J. Inoue and T. Kawazoe, "Nonlinear propagation characteristics of sub-picosecond optical pulses in semiconductor optical amplifiers," 9th European Conference on Integrated Optics and Technical Exhibition, ECIO'99, Torino-Italy, April 13-16, pp. 455-458, 1999.
- [9] M. Y. Hong, Y. H. Chang, A. Dienes, J. P. Heritage, P. J. Delfyett, Sol Dijaili, and F. G. Patterson, "Femtosecond self- and cross-phase modulation in semiconductor laser amplifiers," *IEEE J. Sel. Top Quantum Electron.*, vol. 2, pp. 523-539, 1996.
- [10] N. K. Das, H. Kawaguchi, and K. Alameh, *Advances in Optical Amplifiers*, Paul Urquhart (Ed.), "Ch. 6: Impact of pump-probe time delay on the four-wave mixing conversion efficiency in SOAs", InTech, Austria, 2011.
- [11] M. Razaghi, A. Ahmadi, and M. J. Connelly, "Comprehensive finite-difference time-dependent beam propagation model of counter propagating picosecond pulses in a semiconductor optical amplifier," *IEEE/OSA J. Lightwave Technol.*, vol. 27, pp. 3162-3174, 2009.